Next Materials 9 (2025) 100901

Contents lists available at ScienceDirect

Next Materials

journal homepage: www.sciencedirect.com/journal/next-materials

Research article

Correlation of anomalies in temperature dependences of electrical resistance and thermal deformation of $YBa_2Cu_3O_{7-\delta}$ ceramics

A.E. Rabadanova [a], D.K. Palchaev [a,*], V.S. Efimchenko [b], R.M. Emirov [a], Sh.P. Faradzhev [a], S.Kh. Gadzhimagomedov [a], Zh.Kh. Murlieva [a], M.Kh. Rabadanov [a], S.V. Simonov [b], A.M. Aliyev [c], A.A. Antsiferova [d,e], M.E. Iskhakov [a], N.M.-R. Alikhanov [a]

[a] Dagestan State University, Makhachkala 367008, Russia
[b] Institute of Solid State Physics, of RAS Chernogolovka, 142432, Russia
[c] Amirkhanov Institute of Physics of DFRC of RAS, Makhachkala 367003, Russia
[d] National Research Center "Kurchatov Institute", Moscow 123182, Russia
[e] Moscow Institute of Physics and Technologies, Dolgoprudny, Moscow 141700, Russia

ARTICLE INFO

Keywords:
YBCO
Superconductors
Ceramics
Structure
Electrical resistance
Thermal expansion
Correlation

ABSTRACT

Direct measurements of the temperature dependences of the electrical resistance and the thermal deformation of the lattice parameters in microcrystalline $YBa_2Cu_3O_{7-\delta}$ (YBCO) with two dominant superconducting phases (DSPs) were carried out in the normal state and in the temperature range of superconducting transition ($\Delta T_c \sim$ 10 K). The presence of a linear correlation between the temperature coefficients of electrical resistance (TCR) and the thermal (volume) expansion (TEC) was shown – below (is direct) and above (is reverse) the temperature of the transition to the pseudogap state ($\sim$ 160 K) with a correlation coefficient of no less than 0.98. As it established from the dependences of the derivatives of resistance on temperature for each of these phases the temperature dependences of the lattice parameters demonstrated discontinuity in the region of average values of the transition temperatures to the superconducting state ($T_c \approx$ 90.5 K and $T_c \approx$ 87 K). Deviations from the zero TCR value for these phases at mid-T_c were positive and changes in TEC of all lattice parameters at these temperatures occurred to be with sign inversion. The scenario for the phenomena of charge excitations in YBCO and their pairing associated with anomalous compression of the volume of lattice upon cooling to T_c and its subsequent positive striction directly in T_c in the absence of a magnetic field is present.

1. Introduction

High-temperature superconductors (HTSC) including YBCO are promising materials for the creation of second and third generation superconductors [1,2], memristors [3], quantum computers [4–6] and others. Knowledge of the true nature of the formation of their properties can significantly increase the efficiency of endowing these materials with the characteristics in practical demand. At the same time, the essence of the nature of the HTSC phenomenon remains to be one of the unsolved problems in modern physics [7–11], since conductivity and even superconductivity are observed in non-metals, which are strongly correlated electron systems.

Unlike metals, concerning HTSC it makes sense to speak only about some local elementary charge excitations (ECE) in interacting atoms with an insignificant degree of their socialization due to their obvious interactions via the lattice. Moreover, it is not clear what the "formation of an energy gap" means in this case because of the pairing of quasiparticles that arise as a result of doping determining the order parameter. In this regard, it is obvious that to solve these issues it is necessary to understand the nature of the origin of charge excitations and their relaxation processes in non-metals. It is necessary to take into account that charge excitations are the same quasiparticles such as fermions, similar to elementary excitations of electrons, induced in the neighboring atoms.

An important milestone in this understanding was the BCS theory, which emphasized the role of the coupling of ECE (electrons) and elastic excitations (phonons) of the atomic and electron subsystem for low-temperature superconductors. The presence of bound state of two quasiparticles interacting via a virtual phonon implies a vanishingly small elastic deformation of the lattice. This is possible only at quasi-harmonic

* Correspondence to: The Republic of Dagestan, Dagestan State University, Gadzhiyev, Street, building 43-a, Makhachkala 367000, Russia.
E-mail address: dairpalchaev@mail.ru (D.K. Palchaev).

https://doi.org/10.1016/j.nxmate.2025.100901
Received 24 December 2024; Received in revised form 30 June 2025; Accepted 30 June 2025
Available online 8 August 2025

oscillations close to harmonic ones and temperatures close to 0 K. Quasi-harmonic oscillations at $T \neq 0$ K can occur only in loosely packed structures, which are characterized by the inversion of the sign of TEC (corresponding to anharmonicity). The anharmonicity of oscillations, which ensures the change in the elasticity of the bond between atoms, excludes the birth of a virtual phonon and determines the dependence of resistance on the temperature [12]. The main problem of the theory [12], associated with the impossibility of quantitative description of the phonon electrical resistance even of classical metals, is the lack of knowledge about the dependence of the deformation potential on the temperature, which determines the screening of the lattice ions. Socialized electrons in metals with the constant concentration provide such screening.

According to [12] the anharmonicity has a direct relation to the formation of the thermal deformation potential, i.e., to the lattice expansion or contraction due to the free energy loss. The resistance value depends not only on the temperature change but also on the volume $\rho(T,V)$ during the transition to a new equilibrium state at a constant pressure. Note that the change in free energy when interpreting the temperature dependence of resistance of both nonmetals and metals is still neglected [13–19] because of the smallness of the change in volume. The volume changes by less than ~10 % from 0 K to the melting temperature. Whereas, in the quasi-static process of transition of the system from one equilibrium state to another, the value of TEC changes by many orders of magnitude in this temperature range.

Earlier in [20,21], the constancy of the relation was shown:

$$\rho(T,V)/\beta(T,V)\cdot T = \rho^* \quad (1)$$

for each equilibrium state of metals, where $\beta(T,V)$ – TEC; $\beta(T,V)\cdot T = [dV(T)/V(T)dT]\cdot T$. The characteristic resistivity ρ^* is ~ 10^{-6} Om·m for more than thirty classical conductors, including phases with magnetic and atomic ordering [20–24]. The Pearson's correlation coefficient (PCC) between the temperature dependences $\rho(T,V)$ and $\beta(T,V)\cdot T$ from the temperatures close to 0 K to the melting temperature is ~0.999, indicating the closeness of this relationship to a functional one. Note the changes in each of the parameters $\rho(T,V)$ and the thermodynamic complex $\beta(T,V)\cdot T$ are six or more orders of magnitude, and the change in ρ^* of the corresponding phase does not exceed the total error of their determination. The linear relationship (1) between these parameters shows that at $T \neq 0$ K the value of $\rho(T,V) \to 0$, when $\beta(T) \to 0$. Note also that the trend $\beta(T) \to 0$ or $\beta(T) < 0$ below T_c is observed for both low-temperature and high-temperature superconductors [25–27].

Classical metals with predominantly metallic bonding are not superconductors, whereas the probability of superconductivity and the values of their T_c increase with an increase of the proportion of covalent bonding. For non-metallic conductors, relative thermal deformation is usually accompanied by the occurrence of the charge excitations, for example, in semiconductors. Therefore, one should expect the relationship between the temperature coefficient of electrical resistance (TCR) $\alpha_\rho = d\rho/\rho dT$ and (TEC) $\alpha_V = dV/VdT$ in non-metals, in contrast to classical metals.

The existence of the lattice thermal deformation anomaly near T_c confirmed by the results not only for YBCO [28–37], but also for other HTSCs [38–42]. In particular, the authors of [29] found that the dependences of the ***c*** parameter and volume on temperature of optimally doped YBCO in the absence of a magnetic field exhibit a 'break' with a positive jump of ~ 3 % immediately at T_c. Prior to this jump, lattice compression occurs up to T_c. Other authors [31,35] have shown that the superconducting transition is accompanied by a critical behavior of the thermal expansion coefficients of the parameters a and b, i.e. a critical lattice deformation near T_c.

The results presented in [28–37] performed immediately after the discovery of superconductivity in both YBCO and other HTSCs [38–42]. The neglect of the significance of the lattice thermal deformation effect in interpreting the conductivity of these materials was apparently due to the persistent view of the insignificance of the volume change.

Although in the same years it was shown in [28] that the absolute volume deformation (compression) of the YBCO lattice by only ~ 1.6 % caused by an increase in the content of labile oxygen ($\delta \leq 1$) at constant values of temperature (~5 K) and pressure (~1 atm) leads to a transition from the dielectric state to the superconductor state with T_c ~92 K. The authors [43–46] tried to relate the mechanism of superconductivity formation in yttrium and bismuth cuprates to lattice deformation by changing their doping level. Particular attention was paid to the change of local structure in CuO_2 planes, which are mainly superconducting. These planes have features of curvature, which occur when Cu atoms are displaced toward the apical oxygen relative to these planes. These Cu atoms with oxygen atoms located in the ***a*** and ***b*** directions at the corners of the CuO_2 plane form triangles. As a result of the careful calculations of chemical bond lengths, it was found that all six parameters characterizing these triangles are stable and do not depend on the degree of doping, from what the stability of the area formed by the bases of these triangles follows. The results of [43–46] indicate the relationship between the doping level and the lattice deformation, which provides the superconducting state. This is in the agreement with the resistance aspiration to zero at vanishingly small deformation of the conductor lattice, which is evident from the linear correlation (1) of the temperature dependences of the athermal resistance $\rho(T)/T$ and β(T).

Previously, we [47] showed the presence of a linear relationship between the doping level (***p***) and TCR for 20 nanostructured superconducting ceramics based on YBCO, regardless of their porosity and particle dispersion, as well as changes in the nature of conductivity. This relationship follows from the similarity of the dependences of the average values of ***p*** and TCR on ΔT_c.

In the present work, for the first time the connection between the conductivity of HTSPs and lattice strain is considered at the example of YBCO. Perhaps, this can bring us closer to understanding the nature of conduction, high-temperature superconductivity [9], the conduction of "strange metals" [10] and metals with saturated electrical resistance [11]. Obviously, to establish this connection, first of all, we should investigate the correlations of the temperature coefficients of electrical resistance and thermal expansion for the same YBCO sample in the normal state and in the temperature range of the superconducting transition.

For this purpose, the temperature dependences of the electrical resistance and thermal expansion of microcrystalline YBCO in the normal phase and during its transition to the superconducting state in a zero magnetic field have been investigated. We have put forward the hypothesis on the possible mechanisms of the occurrence of charge excitations during lattice compression upon cooling to T_c and their pairing, the "trigger" of which is positive striction at T_c.

2. Experiment

A microcrystalline sample of $YBa_2Cu_3O_{7-\delta}$ was prepared by solid phase sintering using Y_2O_3 (~99.9 %), $BaCO_3$ (~99.9 %) and CuO (~99.9 %) taken in a molar ratio of 1:2:3 by metals according to the following reaction:

$$Y_2O_3 + 4BaCO_3 + 6CuO \rightarrow 2\ YBa_2Cu_3O_{7-\delta} + 4CO_2\uparrow \quad (2)$$

The components with the addition of ethyl alcohol were mixed in an agate mortar and pressed under ~100 MPa. Synthesis and sintering of the samples were carried out in air in 3 steps of about 10 h in each one. Synthesis of the compound with up to ~ 90 % YBCO took place at ~ 870 °C (confirmed by thermal analysis). The sintering (know-how) at low temperatures of 900 °C and 909 °C was ensured by the fact that the starting powder consisted of nano- and microcrystals. The amount of YBCO phase in the ceramics increased up to ~95 % and crystallites grew in the c direction during sintering. The heating rates to the synthesis and sintering temperature were about 2 °C/min, and the cooling rate to 450

°C was about 1.5 °C/min. Oxygen saturation of the ceramics was carried out in air at 450 °C for 5 h, and then the furnace was turned off. The density of the sample after sintering at ~909 °C was 5.9 g/cm^3. The samples were made from this ceramics for electrical resistivity and heat capacity studies, and powder was obtained from the residue for structure studies. The analysis of four samples, with insignificant variations of sintering temperature, obtained by the developed technology, showed the reproducibility of their structure and properties.

The resistance of a 4 × 2 × 1 mm sample was measured using the four-probe method in automatic mode on a setup containing a Keithley 2002 multimeter controlled by an SR830 nanovoltmeter for current switching and a PTC 10 for temperature control. The setup is fully automated and allows current-switched $\rho(T)$ measurements over a temperature range from 80 to 300 K. The control program is written using the LabView software package. Ohmic contacts of potential copper probes were attached to the sample in its center at a distance of ~1.5 mm with SP-40 plus silver paste. Current contacts were attached to the two opposite side faces of the sample with the same paste at a distance of ~4 mm. The temperature of the sapphire substrate on which the sample was fixed with BF-2 adhesive is measured using a copper-constantane thermocouple. The sapphire substrate with a diameter of ~ 10 mm and a thickness of ~ 3.5 mm, cooled with helium gas in a sealed chamber of a nitrogen cryostat, served as a "thermostat" for the sample. The temperature dependence of thermal expansion in the temperature range from ~ 82 K to 300 K was established on the basis of lattice parameters obtained on a SIEMENS D-500 diffractometer equipped with a low-temperature cryostat. The sample was loaded at room temperature with subsequent cooling to nitrogen temperatures. The shooting was carried out on a substrate made of monocrystalline silicon with the cell sized for the sample of 15 × 20 mm. Scanning was carried out using CuK$\alpha_{1,2}$ X-ray radiation in the scheme with a secondary monochromator in the range of 2θ angles from 5 to 90° (or 5–50°) with a step of 0.02° and an exposure of 12 s at each point. High Score plus software was used for calculations.

3. Results

The study of the temperature dependence of electrical resistance was carried out in the quasi-static mode of heating of a preliminary thermostatted sample at the boiling point of nitrogen at a rate of 0.015 K/s. Fig. 1 shows the $\rho(T)$ dependence of the studied sample, where the temperatures of the transition to the pseudogap (T^* ~ 160 K) and superconducting states are indicated. There is a slight increase in the slope of the almost T-linear dependence upon transition to a pseudogap

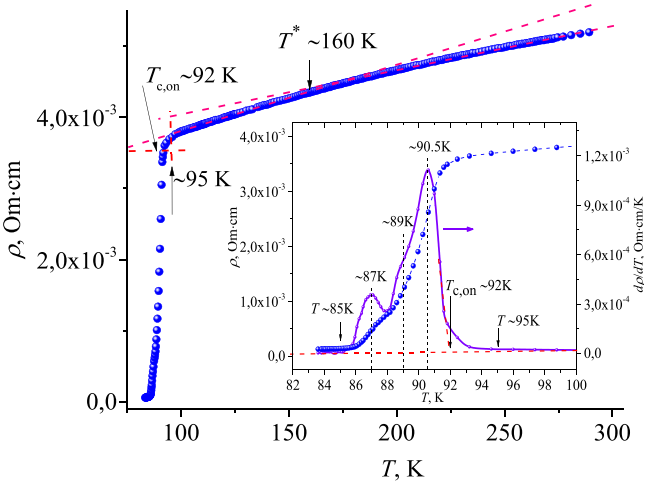

Fig. 1. Dependence of electrical resistance on temperature. Inset are $\rho(T)$ and $d\rho/dT$ from T in the region of transition to the superconducting state.

state at the dependence of the electrical resistance of a microcrystalline sample on the temperature, in contrast to a single crystal [48–50]. This indicates that the conductivity increases without typical to single crystals [51] obvious structural changes due to the polycrystallinity of our sample. Fig. 1 shows the temperature range where the resistance decreases to the temperature of the onset of the transition ($T_{c,\,on}$), which is usually observed for such dependences. The onset of the transition to the superconducting state occurs at ~ 92 K, which corresponds to the T_c value for the optimally doped phase. The transition width (ΔT_c) is equal to ~ 7 K. A deviation from regularity such as a "shoulder" is observed at ~ 89 K in the region of the superconducting transition (inserted at Fig. 1) on the dependence $d\rho/dT = f(T)$ determining the middle values of T_c, in addition to two well-resolved peaks (90.5 K and 87 K). The presence of the "shoulder" in the interval from 90.5 K to 87 K indicates the existence of other non-dominant superconducting phases in this temperature range. Moreover, a wide interval of the transition ΔT_c and a large width of individual peaks also indicate the multiphase nature of the samples in terms of oxygen content. In this regard, a large width of dominant anomalies on the temperature dependences of thermal expansion and heat capacity, manifested as a singularity in T_c, is to be expected.

The results of the experimental studies of the heat capacity normalized over temperature (C_p/T) in the range of 20 – 160 K are present at Fig. 2. The values of $C_p(T)/T$ decrease monotonically on 3 J/(kg·K) with decreasing temperature from 160 K to 20 K. The inset (Fig. 2a) shows an enlarged fragment of the anomaly observed within the dependence $C_p/T = f(T)$ at the region of the superconducting transition. The anomaly of the excess of the electron component over the phonon component in the range from ~ 92 K to 85 K (ΔT ~ 7 K) determined by the change in the density of states near the Fermi surface is consistent with the results of the dependence of $d\rho/dT$ on T (see Fig. 1).

The anomalous deviations from the regular temperature dependence of the heat capacity typical for the DSPs were approximated using the Lorentz function and transformed into individual peaks (Fig. 2b). The use of the Lorentz function was due to the fact that the width of the peaks implies the presence of subphases in the dominant phase. The most intense peaks are observed at temperatures of ~ 90.5, 89.3, 88.7, and 87.4 K, which mainly coincide with the deviations from regularity on the $d\rho/dT$=$f(T)$ dependence. Using this dependence, the Tc temperatures including the onset of the transition at ~ 92 K were refined for different DCPs of the studied sample.

The results of the study of the structure such as the diffraction pattern of the powder from ground ceramics in the range from 300 K to 82 K shown at Fig. 3. This powder consists of particles with signs of texture growing towards the ***c*** direction. The parameter ***c*** was determined by the positions of the diffraction peaks from the planes [002], [003], [005], [006]. The structural analysis was carried out using the crystal structure model from the database (PDF-2) No. 98–003–9359 for the space group Pmmm: Y (½½½), Ba (½½ 0.1851), Cu1 (0 0 0.3557), Cu2 (0 0 0), O1 (0 ½ 0), O2 (0 ½ 0.3778), O3 (½ 0 0.3776), O4 (0 0 0.1600) [52].

The analysis allowed for the determination (Fig. 4) the following divergence coefficients: weighted profile ωRp = 5.07 %; profile R_p = 3.7433 %; "goodness of the fit" χ^2 = 1.39; Bragg coefficient R_B = 3.64 %. The following values of the crystal cell parameters were obtained using the Ritveld method: ***a*** = 3.82361 Å; ***b*** = 3.88624 Å; ***c*** = 11.68546 Å; **V** = 173.6397 Å^3. The crystallographic density of the unit cell is 6.353 g/cm^3. Along with the diffraction peaks of the $YBa_2Cu_3O_{7-\delta}$ main phase Fig. 4 contains minor peaks corresponding to the Y_2BaCuO_5 (Y-211) and $BaCuO_2$ impurity phases, whose content does not exceed ~ 3 %.The oxygen index for $YBa_2Cu_3O_{7-\delta}$, determined from the empirical relationship: $y = 7 - \delta = 75.25 - 5.856 \cdot \boldsymbol{c}$, is ~ 6.9. This index is close by magnitude to the oxygen content (~ 6.83) established from the T_c value for this sample using electrical resistance data. Such a high y value is an indicator of the optimal oxygen content in the YBCO

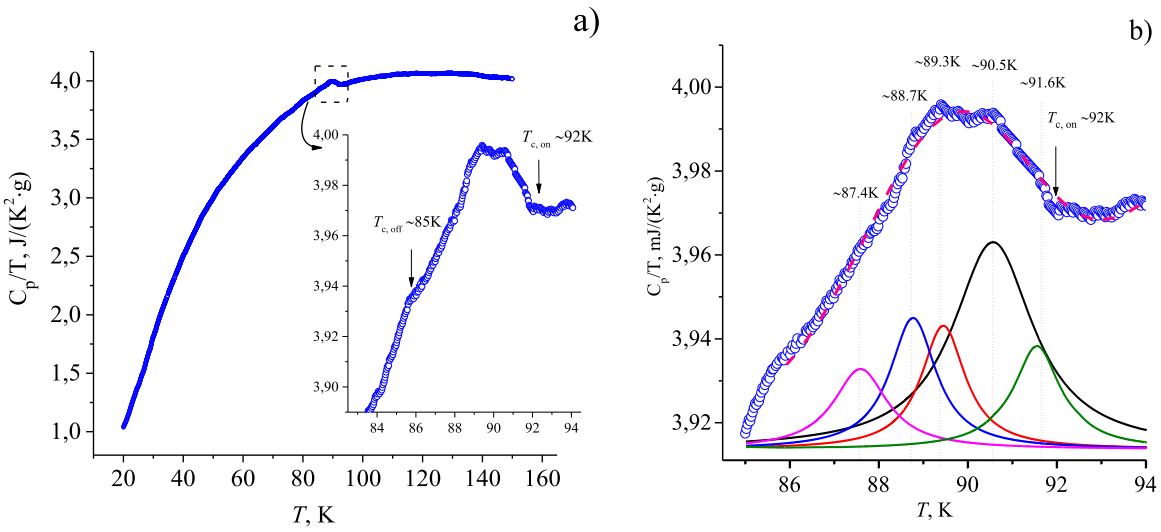

Fig. 2. Dependence of heat capacity on temperature. Results of T_c observed in the $\rho(T)$ dependence (Fig. 1) are refined for different DCP (Fig. 2b).

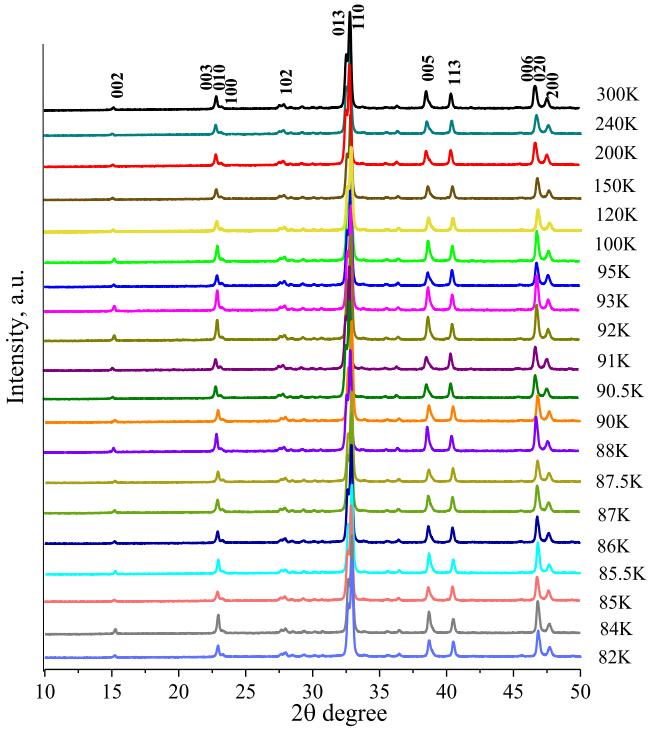

Fig. 3. X-ray diffraction patterns of YBCO sample at different temperatures.

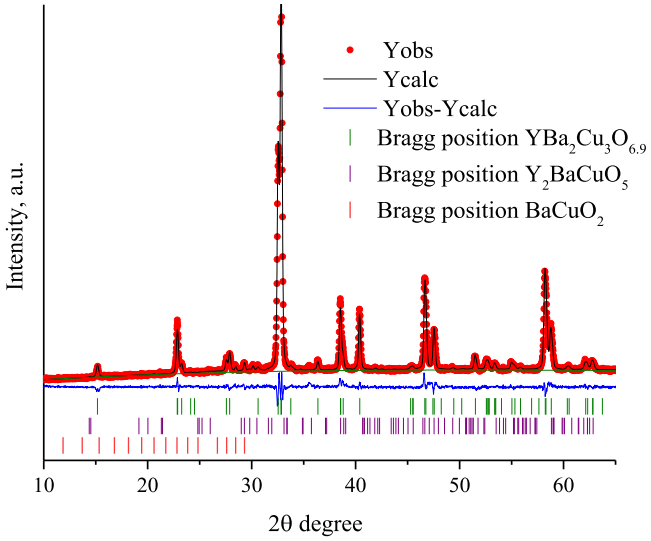

Fig. 4. Experimental (red), calculated (black) and differential (blue) diffraction patterns at the room temperature.

structure with almost completely occupied O(1) positions in the CuO chains along the ***b*** axis. The ratio of the intensities of reflections from the [(006) (020)] and (200) planes at Figs. 3 and 4 confirms the ordering of oxygen atoms into the ***b*** direction.

Fig. 5 demonstrates the change in the position of the peaks (005) and [(006)+ (020)] of the $YBa_2Cu_3O_{7-\delta}$ superconducting phase depending on the temperature. The blurring of the peaks indicates the presence of other phases in the sample that are close to this phase in oxygen content. A shift in the peaks of the $YBa_2Cu_3O_{7-\delta}$ phase towards larger angles indicating lattice compression is observed when the temperature is reduced up to ~ 92 K. A sharp shift in the opposite direction occurs at the temperatures below ~ 90.5 K. It indicates an increase in the values of the parameter ***c*** at the superconducting state. A reverse in the direction of the ***c*** parameter change occurs in the temperature range of 90.5 — 87 K, which corresponds to the midpoint values of the transition to the superconducting state according to electrical resistance data.

Table 1 summarizes the values of the lattice and volume parameters and the temperature coefficients of expansion of these parameters for the studied sample. Fig. 6a shows the average temperature dependences of the volume $V(T)$ and the lattice parameters $\boldsymbol{c}(T)$, $\boldsymbol{a}(T)$ and $\boldsymbol{b}(T)$ over the microcrystalline sample within the temperature range from 300 K to the superconducting transition as well as in the ΔT_c range of this transition with predominance of two phases with different T_c values. The ΔT_c range of ~ 7 K (from ~ 92 to ~ 85 K) where anomalies appear in the $V(T)$ dependence (Fig. 6a) is consistent with the ΔT_c value following the temperature dependences $d\rho(T)/dT$ (Fig. 1) and $C_p(T)/T$ (Fig. 2). The effect of positive striction of the volume of the two main superconducting phases is observed in the temperature ranges of ~ 92 K to ~ 90 K and from ~ 88 K to ~ 87 K, respectively. There are extrema on the dependences of the thermal expansion coefficients TEC $\alpha_{\boldsymbol{V}}(T)$, $\alpha_{\boldsymbol{c}}(T)$, $\alpha_{\boldsymbol{a}}(T)$, $\alpha_{\boldsymbol{b}}(T)$ (Fig. 6b) and electrical conductivity $d\rho(T)/dT$ in the similar regions at $T_c \approx 90.5$ K and $T_c \approx 87$ K (Fig. 1). The coefficients $\alpha_{\boldsymbol{V}}(T)$, $\alpha_{\boldsymbol{c}}(T)$, $\alpha_{\boldsymbol{a}}(T)$, $\alpha_{\boldsymbol{b}}(T)$ deviate from their zero values (Fig. 6b) with sign inversion within the transition region. The temperature dependences

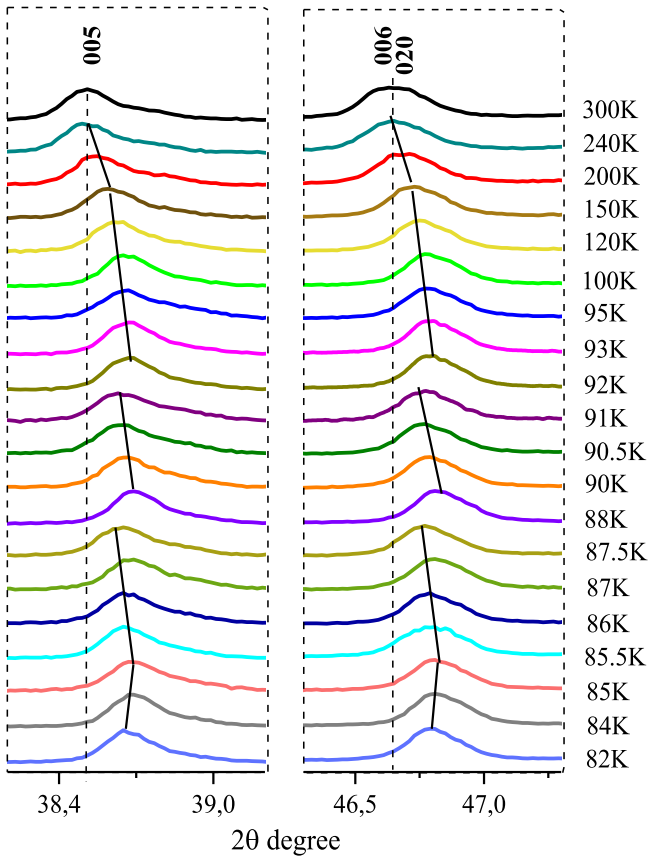

Fig. 5. Effects of shifting the maxima of peaks 005, 006 and 020 in the range from room temperature to 82 K.

$\alpha_V(T)$, $\alpha_c(T)$, $\alpha_a(T)$, $\alpha_b(T)$ were determined from the experimental data (21 points) and shown at Fig. 6a. Directly at the transition temperature ($T_c \approx 90.5$ K), the extremum of the $\alpha_V(T)$ dependence has a negative sign, whereas the extremum of the $d\rho(T)/dT$ dependence at this temperature is positive (see the inset in Fig. 1). The visual perception of the equality of the coefficients $\alpha_V(T)$, $\alpha_c(T)$, $\alpha_a(T)$ $\alpha_{\boldsymbol{b}}(T)$ as zero at $T > 95$ K is due to the fact that their values in this temperature range are approximately two orders of magnitude smaller than in the $T < 95$ K range.

All points on the temperature dependences of the YBCO lattice parameters (Fig. 6a) correspond to their values in the equilibrium state. The transition to such a state at heating occurs with an increase in entropy due to thermal excitation of first the electronic and then the atomic subsystems. At cooling, the transition to these equilibrium states obviously occurs with the increase of the entropy of quantum chaotization of the electron subsystem and with the increase of the elastic coupling forces between atoms. Note that the resulting entropy of the system is the sum of the contributions of the atomic and electronic subsystems. In turn, the entropy of the electronic subsystem is the sum of the contributions of quantum and thermal chaotization. Thus, the removal of atoms occurs by increasing the thermal chaos of the electronic subsystem, and the lattice compression leads to an increase in its quantum chaos. Thus, the transition to the equilibrium state always occurs with the increase in the corresponding contribution to the resulting entropy. The entropy of quantum chaotization of the electron subsystem reaches a maximum at the temperatures close to 0 K, when the volume is nearly constant. While thermal excitation of this subsystem leads to thermal chaos of electrons near the Fermi level and a corresponding increase in the entropy of the atomic subsystem. The socialization of charge excitations occurs with their appropriate modification by doping in the systems with covalent bonds where conductivity and superconductivity are observed. The information given in [43–46] about the presence of "fixed triangles" in the corrugated planes of CuO_2 superconducting cuprates indicates that the bonds between Cu and O atoms are directed and saturated. Saturation is carried out by additional charge excitations in the polarized atoms providing detailed charge equilibrium. Directionality and saturation leads to some degree of covalency. This is confirmed in [53], according to which the ionic model leads to a good agreement of calculation results with the experimental fact of localization of positive conductivity charges on the CuO_2 plane at taking into account such excitations.

Doping of YBCO with oxygen atoms at a constant temperature, which delivers it the property of superconductivity [28], is accompanied by deformations of the same order as in the Fig. 6a. In the normal state, the estimates of the anisotropy of deformations of the parameters V, $\boldsymbol{c}$, $\boldsymbol{b}$ and $\boldsymbol{a}$ (in percentage) and their average relative deformations per degree occurred to be: (-0.7 % and $35{\cdot}10^{-6}$ K^{-1}); (-0.24 % and $12{\cdot}10^{-6}$ K^{-1}); (-0.3 % and $17{\cdot}10^{-6}$ K^{-1}); (-0.11 % and $1{\cdot}10^{-6}$ K^{-1}) respectively. In this state (Fig. 6a), the change of the $\boldsymbol{a}$ parameter over the entire temperature range is three times less than the change in the $\boldsymbol{b}$. The temperature dependences of these parameters are opposite in the temperature range from 300 K to 95 K, where the T-linear dependence for electrical resistance up to 160 K and a dependence corresponding to a pseudogap state

Table 1
The values of the lattice parameters, volume and the temperature coefficients of expansion of these parameters.

T, K	a, Å	b, Å	c, Å	V, Å^3	α_a [$10^{-3}K^{-1}$]	α_b [$10^{-3}K^{-1}$]	α_c[$10^{-3}K^{-1}$]	α_V [$10^{-3}K^{-1}$]
300	3,82361	3,88624	11,68546	173,63972	4,35888E−5	0,03311	0,00428	0,03743
240	3,8236	3,87852	11,68246	173,24972	9,69854E−4	0,02384	0,00706	0,03187
200	3,82331	3,87627	11,67786	173,06799	0,00539	0,0126	0,0164	0,03436
150	3,82161	3,8742	11,66446	172,7005	0,01055	0,00913	0,01863	0,0383
120	3,82021	3,87332	11,65946	172,52416	0,01226	0,00785	0,01144	0,03153
100	3,81927	3,87269	11,65746	172,42413	0,01575	−0,07004	0,02689	−0,02741
95	3,8189	3,87556	11,65483	172,49639	0,02439	0,2406	0,04072	0,30559
93,2	3,8187	3,87117	11,65407	172,28061	0,14463	0,42049	0,32559	0,89226
92	3,81751	3,87019	11,64547	172,05554	−0,02467	−0,41256	0,02132	−0,41278
91	3,81869	3,8742	11,65213	172,38514	−0,36924	−1,08022	−1,01183	−2,41237
90,5	3,81951	3,87638	11,66059	172,6362	0,39621	−5,6625	−0,1861	−5,45927
90	3,81718	3,89615	11,65431	173,32761	0,45409	−1,90059	0,84926	−0,62917
89	3,81838	3,87142	11,64708	172,16289	0,0275	3,61237	0,38186	4,02599
88	3,81697	3,86818	11,64541	171,94136	−0,55934	−0,39295	−0,75523	−1,70283
87,5	3,81981	3,87132	11,65504	172,34491	−0,15271	−5,16878	−0,52166	−5,83442
87	3,81755	3,88819	11,65149	172,94689	0,25715	−2,6902	−0,09548	−2,54038
86	3,8201	3,87537	11,66081	172,62163	−0,26395	2,71974	0,36726	2,80949
85,5	3,81983	3,87124	11,65187	172,29928	0,69811	3,29352	0,63037	4,6853
85	3,81743	3,86262	11,65347	171,81436	0,65795	0,99155	0,13816	1833
84	3,81721	3,8722	11,64705	172,15434	0,07597	−1,04075	0,30974	−0,71303
82	3,8165	3,86916	11,64546	171,96538	0,09345	0,39285	0,06827	0,5494

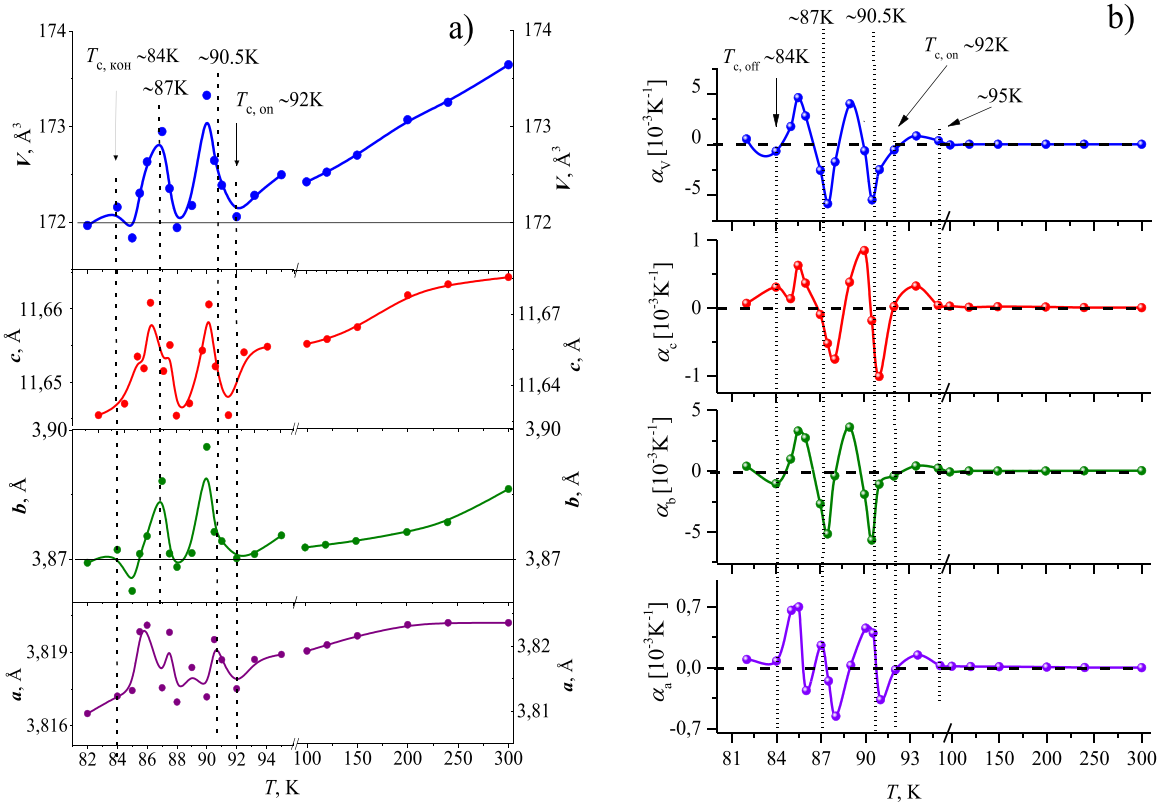

Fig. 6. Temperature dependences of the lattice parameters of the YBCO unit cell and TEC of these parameters.

below 160 K are observed. The compression (volume change by 0.25 %) is observed for all parameters directly in the region of the transition (~ 92 K) to the superconducting state beginning of one of the DSPs (Fig. 6a), which is followed by a sharp increase by more than two times. The temperature ($T_c \approx 90.5$ K) accounting to the midpoint of the interval of this increase for the ***b***, ***c*** and *V* parameters agrees with the established for this DSP from $\rho(T)$ dependence value. The absence of a clear resolution of this feature for the ***a*** parameter is apparently due to the fact that its change is an order of magnitude smaller than the change in the ***b*** parameter. As can be seen (Fig. 6a), the minimum volume value of 172 Å^3, which the lattice had at its compression at the beginning of the transition to the superconducting state, practically does not change with decreasing temperature.

The estimates of the anisotropy of the absolute deformation in percent (%) and the average relative deformations per degree for the *V*, ***c***, ***b*** and ***a*** parameters during the transition to the superconducting state, occurred to be: (0.75 % and $-5{\cdot}10^{-3}$ K^{-1}); (0.013 % and $-8{\cdot}10^{-6}$ K^{-1}); (0.7 % and $-4.6{\cdot}10^{-3}$ K^{-1}); (0.005 % and $-3{\cdot}10^{-5}$ K^{-1}) respectively. Here, the decisive role in the changing ***V*** belongs to the change in the ***b*** parameter. Moreover, the change in Δ***b*** (Fig. 6a, solid line) is practically equal to zero if we do not take into account the effects associated with the superconducting transition of each of the phases. The decisive role of the ***b*** parameter in the formation of the temperature dependence in the region of the transition to the superconducting state is also evident from the TEC data at Fig. 7b, where $\alpha_b(T)$ as well as $\alpha_V(T)$, are approximately five times higher than $\alpha_c(T)$ and $\alpha_a(T)$. The values of $\alpha_V(T)$, $\alpha_c(T)$, $\alpha_a(T)$, $\alpha_b(T)$ in the normal state are two orders of magnitude lower than in the interval of the transition to the superconducting state.

The changes in volume in the temperature ranges of ~ 200 K (in the normal state) and 1.5 K (jump) during the transition to the

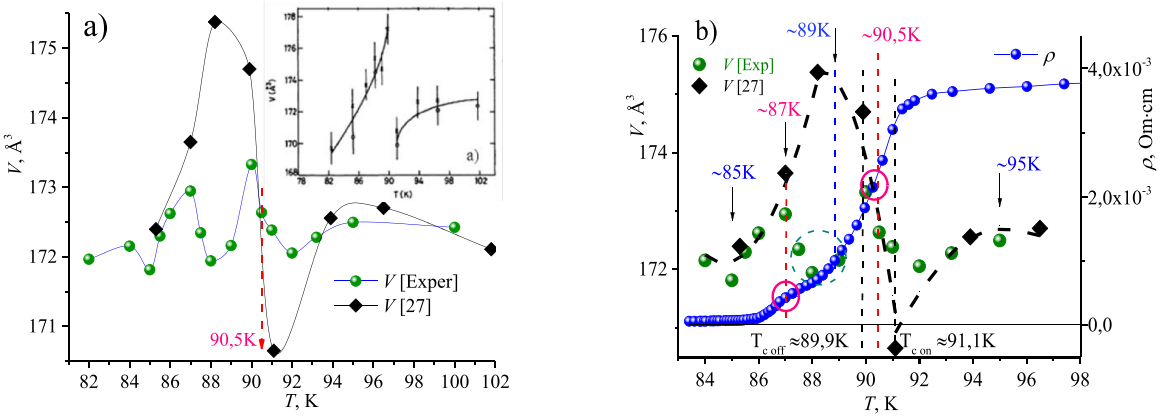

Fig. 7. Temperature dependences of electrical resistance and volumes of our sample as well as from table [27] directly in the region of transition to the superconducting state.

superconducting state DSP (~ 90.5 K) are approximately equal in absolute value and opposite in sign according to Fig. 6a. The transitions of the dominant phases to the superconducting state (Fig. 6a) are presented as a positive deviation of the volumes from a constant value and the derivative of the temperature dependence of electrical resistance over the temperature $d\rho(T)/dT$ (in the inset of Fig. 1).

Fig. 7 shows the anomalies in the dependences of the volume on the temperature of our sample directly in the region of the transition to the superconducting state (green balls) in comparison with the results (black squares) from [29]. The inset (Fig. 7a) demonstrates the discontinuity of the $V(T)$ dependence at the superconducting transition observed in this study. Such a comparison was possible due to the approximate equality of the T_c value for our sample (~90.5 K) determined from the electrical resistance and the sample from [29], where it was established from the diamagnetic susceptibility. The temperature dependences of the lattice parameters of the YBCO sample in the form of powder in [29] were determined from the change in the position of the peaks in the diffraction pattern from the (013) and [(110), (103)] planes. Our dependence is constructed based on sixteen $V(T)$ values, while there are only seven of these values in the corresponding table from [29]. The ceramics from which the powder sample was obtained (seven more points in the inset of Fig. 7a) was additionally studied for achievement of a better resolution of the dependence of the V(T) function in the T_c region; it was single-phase according to [29]. However, we note that the probability of obtaining a single-phase YBCO sample with one superconducting phase is not high, even if it is a small single crystal due to the inevitability of defects in it. Our results show (Fig. 7b) that with a higher resolution (increasing the number of points) of the V(T) dependence in range from 95 K to 85 K, another anomaly could appear at a temperature of ~ 89 K in addition to the anomalies for the two DSFs. This can be seen in the $d\rho(T)/dT$ dependence (insert on Fig. 1).

Fig. 7b shows that the experimental data on $V(T)$ for our optimally doped sample and the sample from [29] fit well to the similar dependence shown in the inset of Fig. 7a. The vertical dashed black lines (Fig. 7b) are drawn through the points of the beginning ($T = 91.1$ K) and the end ($T = 89.9$ K) of the volume jump highlighted in [29]. The average value (red dashed line) between these points is located at temperature of $T_c \approx 90.5$ K. According to our data, for each DSP, the volume decreases by ~0.25 % during the transition to the superconducting state, and according to data from [27] with one DSP, the contraction is ~1.15 %, and then increases sharply between 91.1 K and 89.9 K. As can be seen, the value of $T_c \approx 90.5$ K, obtained in present study for the first DSP based on the results of the electrical resistance study, falls on the right slope of the dependence from [29]. The value of $T_c \approx 87$ K for the second DSP falls on the left slope of this dependence. These temperatures are highlighted by red rings there and below. The green ring highlights the temperature range where T_c of the intermediate superconducting phase is ~ 89 K. The volume decreases (the dotted line in Fig. 7b) so that $\alpha_V = dV(T)/VdT \approx$ constant in the interval from ~ 95 K to the complete transition of our sample to the superconducting state.

Reaching extremes at T_c in the absence of a magnetic field, both when approaching from high and low temperatures, leads to a second-order phase transition with zero entropy difference. Transitions to the equilibrium state to the left and right of T_c at constant pressure and temperature T_c according to the virial theorem [54] should occur with a change in the volume. In this case, the work on an abrupt change in volume occurs due to a change in the internal energy. Experimental facts indicate that the transition from the superconducting state to the normal (disordered) state along with an increase in temperature occurs with an increase in the excitation energy, as is valid for all second-order phase transitions. A sharp increase in volume in T_c leads to a sharp decrease in internal energy. That is, totally it leads to a sharp decrease in the excitation energy of the charge subsystem and establishment of order in it. In YBCO, the transition (Fig. 6a) to the superconducting state is preceded by an anomalous compression of the lattice. The effect of such a compression upon cooling over an interval of only 3 K (Figs. 6a and 7b) can manifest itself only in loosely packed structures. Compression of the lattice of such structures indicates a weakening of the directionality and saturation of the covalent bond ensured by the high inertia of the electrostatic field between the interacting atoms, typical of such a bond. A decrease in the inertia of this field (with a weakening of the bond) leads to an increase in the response of the system to minor external effects. This implies the appearance of additional charge excitations, which are prone to socialization, as evidenced by the increase in conductivity. These charge excitations can be consider as quasiparticles – fermions with the energy spectrum obeyed to the Pauli principle. Compaction of the structure not only increases the socialization of these charge excitations but also decreases the amplitude of thermal vibrations of atoms due to a decrease in anharmonicity upon lattice compression. A slight linear change in the average values of the volume of these phases associated with a decrease in the contribution of the anharmonic component of the amplitude of thermal oscillations is maintained until the complete transition. The volume decrease up to $T_{c,\ on} = 92$ K, apparently, should be considered as a limit of admissible lattice compression, followed by its sharp increase.

The anomaly (Fig. 6a) associated with a 0.75 % volume increase after such a compression results in the decrease in the Fermi wave vector contained in the expression the solution of the Schrödinger equation for quasiparticles. This is consistent with the fact that an energy gap arises in HTSC, which is the larger when the coherence length is smaller. For HTSC, this length is of the order of the interatomic distance. It can be assumed that a pair of quasiparticles (socialized ECEs arising from the weakening of covalent bonds) with antiparallel spins is a Cooper pair. The socialized quasiparticles which characterized by paramagnetism and a sharp deformation of the lattice in T_c leads to the emergence of the gap caused by the antiparallel spin ordering of ECEs at the interatomic distance. This effect is possibly similar to the Villari effect, i.e. under the corresponding deformation, magnetic ordering with a transition from paramagnetism to diamagnetism occurs in YBCO.

The distorted perovskite structure of $BaBiO_3$ was shown [55] to be energetically favorable due to the presence of initially paired electrons and holes in the upper antibonding orbital of Bi6s -O2p_{σ^*} of neighboring octahedral complexes. Doping of this compound changes the lattice distortion and transfers it from the insulator state to the superconductor state. A transition from the insulator state to the superconductor state occurs with a change in the volume of YBCO by only ~1.6 %, because of its doping with oxygen [28]. Obviously, such structures have something in common that ensures their transition from the state of normal conductivity to the superconducting state with small thermal deformations.

The change in the energy of the system with the absolute volume deformation of the lattice of the order of ~ $\Delta V \approx 5$ Å$^3 \approx 5{\cdot}10^{-30}$ m^3 (Fig. 7) directly upon the transition to the superconducting state, according to the virial theorem [54], is of the order of 10^{-5} eV. Such a positive deformation ΔV leads to the decrease of the wave vector and the Fermi level ($2\Delta\varepsilon_F = \hbar^2 (\Delta k)^2/2{\cdot}m$) by ~ 0.4 eV. Taking into account that $2\Delta\varepsilon_F \sim T_c$, it is possible to determine the thermal energy to break a Cooper pair ECE: $\varepsilon \sim k_B{\cdot}90$ K ≈ 0.01 eV. Based on this, we can estimate the proportionality coefficient between $2\Delta\varepsilon_F$ and $k_B{\cdot}T_c$ for YBCO. Its value is of the order of ~ 40, i.e. an order of magnitude greater than that for low-temperature superconductors – 3.5. Thus, our results may indicate the possible applicability of the BCS model for high-temperature superconductors.

Materials with a covalent type of bond have high elasticity therefore in HTSC the probability of the emergence of a virtual phonon is significantly higher than in low-temperature superconductors with a lower proportion of covalence. Apparently, this also explains the presence of high values of T_c for HTSC. In this case, the model adopted in the BCS theory is close to reality in terms of the emergence of a bound state of the ECE of two interacting neighboring atoms through a virtual phonon. A decrease in thermal deformation below T_c means a decrease in the anharmonicity of atomic vibrations in this temperature range and an

increase in the elasticity of the YBCO lattice. The thermal deformation of the lattice (Fig. 6a) immediately after the transition to the superconducting state tends to zero ($\Delta V \rightarrow 0$), i.e. over the entire range $T_c \rightarrow 0$ K the change in volume is vanishingly small. This is the confirmed by the results of the studies on changes in the lattice parameters within this interval [25–27].

4. Correlations

The role of volume change in the formation of superconductivity in YBCO can be substantiated by analyzing the correlation of relative changes in electrical resistance and thermal deformation of the lattice above T_c and in the transition range, since the relative changes in these parameters are orders of magnitude greater than their absolute values. Moreover, they reflect the quantum nature of the change in the elastic component of deformation as well as charge excitations and their relaxation during the transition from one equilibrium state to another. It is determined by the change in the value of the thermal expansion coefficient such as a change in the anharmonicity of atomic vibrations, which is the quantized, and the quantum nature of the change in the excitation energies of quasiparticles.

Fig. 8a – d show the temperature coefficients of resistance $\alpha_\rho = d\rho/\rho dT$ and volume expansion $\alpha_v = dV/VdT$ above and below the transition to the pseudogap state in the ranges from ~ 290 K to ~ 140 K and from ~ 120 K to ~ 95 K as well as the results of the correlation analysis of these dependences. The dependence $\alpha_V(T)$ was obtained from the temperature dependence of the volume established as a result of approximation of the temperature dependences of the ***a***, ***b*** and ***c*** lattice parameters (Fig. 6a), and $\alpha_\rho(T)$ – from the data $\rho(T)$ presented at Fig. 1.

As can be seen, the relationship between $\alpha_V(T)$ and $\alpha_\rho(T)$ are linear with the Pearson's correlation coefficients ~ 0.992 and ~ 0.977 above and below the transition to the pseudogap state temperature (~ 130 K ± 15 K) respectively. The correlation above this temperature is direct as in classical conductors and it is inverse below it as in the intermetallics with saturable resistance. The values of $\alpha_V(T)$ and $\alpha_\rho(T)$ differ (Figs. 8a and 8b) by two orders of magnitude; nevertheless, the correlation of these dependencies is linear with correlation coefficients close to unity.

Fig. 9a - c show the temperature dependences of $d\rho(T)/dT$ and $\alpha_V(T$; $\alpha_\rho(T)$ and $\alpha_V(T)$; $\alpha_\rho(T)/\alpha_\rho{}^*$ and $\alpha_V(T)$ in the region of the superconducting transition, where $\alpha_\rho{}^*$ is the maximum value of $\alpha_\rho(T)$ for each of the phases.

The anomalous deviations of the dependences of $\rho(T)$ at the corresponding temperatures in these Fig. 9 are indicated by circles. The red circles highlight the T_c values for the two dominant phases and the blue ones indicate the T_c values for the weakly manifested superconducting phases in the temperature dependence of $\rho(T)$. The parameter $\alpha_\rho/\alpha_\rho{}^*$ is presented to reveal two superconducting phases in the range from ~ 86 K to ~ 91 K, which are unresolved at Figs. 6b and 9a. The $d\rho(T)/dT$ dependence (Fig. 9a) clearly shows DCPs with T_c ~ 87 K and ~ 90.5 K. The phase with T_c ~ 86 K appears on Fig. 9b and the $\alpha_\rho/\alpha_\rho{}^*$ dependence (Fig. 9c) clearly shows the superconducting phases with T_c ~ 86 K and ~ 89 K, which are poorly manifested at Figs. 1 and 9a. Anomalies in the temperature dependences $d\rho(T)/dT$, αρ(T) and $\alpha_\rho/\alpha_\rho{}^*$ are well resolved due to a large number of $\rho(T)$ values. There are fewer points on the $V(T)$ dependence but the anomalies for the two DCPs observed on the $\rho(T)$ and $V(T)$ curves are in good agreement.

The anomaly of one phase smoothly passes into the anomaly of another phase for multiphase samples (Fig. 9), therefore, exact coincidence of anomalies for all phases after the first one should not be expected. The values of $\alpha_\rho(T)$ are approximately three orders of magnitude higher than those of $\alpha_v(T)$ in the transition interval. Note also that $\alpha_v(T)$ in the normal state is two orders of magnitude lower than in the transition interval. As can be seen, the temperature dependence of electrical resistance is a sensitive parameter to thermal deformation of the lattice. The correlation of $\alpha_\rho(T)$ and $\alpha_v(T)$ indicates the importance of thermal deformation in the formation of $\rho(T)$ in the normal and superconducting

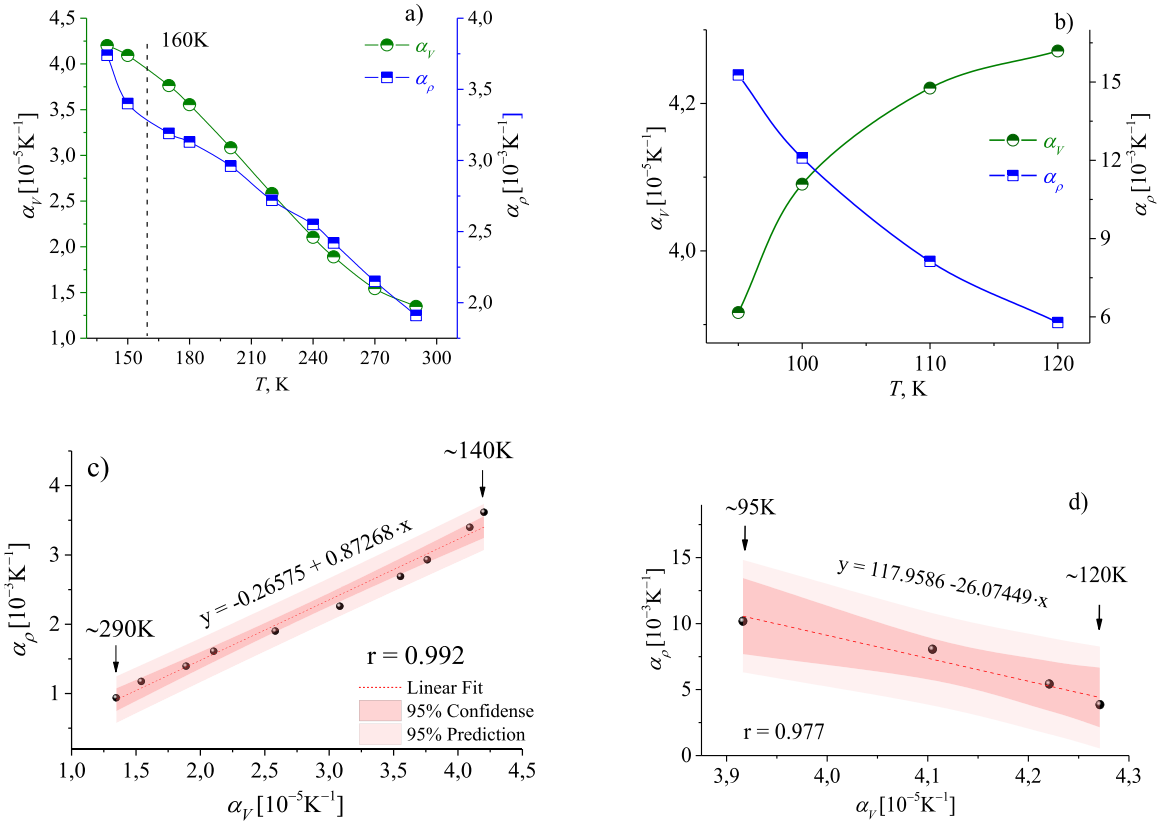

Fig. 8. Dependences $\alpha_V(T)$ and $\alpha_\rho(T)$ – a) and b). Correlations $\alpha_V(T)$ and $\alpha_\rho(T)$ in the normal – c) and pseudogap – d) states.

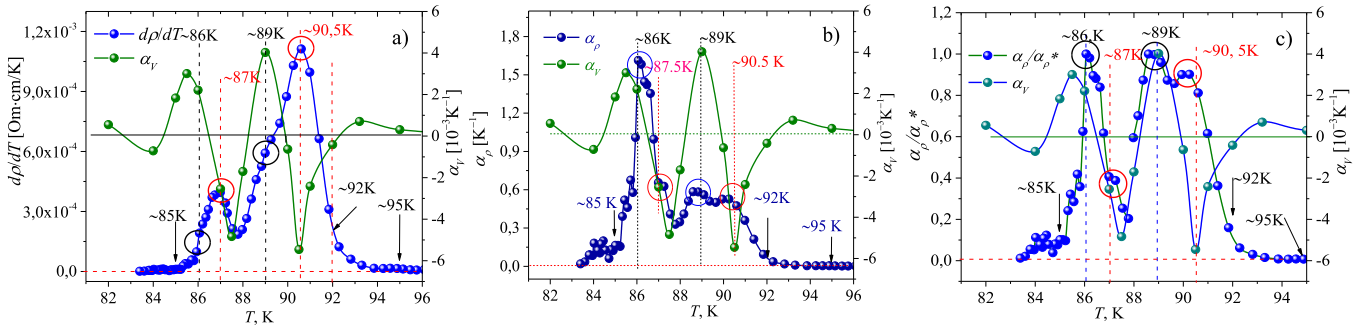

Fig. 9. Temperature dependences: $d\rho(T)/dT$ and $\alpha_V(T)$ – a); $\alpha_\rho(T)$ and $\alpha_V(T)$ – b); $\alpha_\rho(T)/\alpha_\rho{}^*$ and $\alpha_V(T)$ – c) in the region of the superconducting transition.

states.

The emergence of superconductivity occurs with the manifestation of an anomaly of thermal deformation of the lattice as well as its deformation at a constant temperature [28], which takes place with a change in the oxygen content between the sites occupied by copper atoms in the base block. The Meissner-Ochsenfeld effect in a magnetic field occurs with deformation since this transition is a first-order transition. In this regard, the effects of equality of resistance to zero in the superconducting state and the Meissner-Ochsenfeld effect should be the considered from a unified position taking into account the features of the formation of deformation of the HTSC lattice. The effects of excitation and relaxation of the ECE in the system of interacting polarized atoms [54] are accompanied by the performance of work to exit the system from the state of equilibrium and return to a new state after various external influences. According to [56], the detailed charge equilibrium in YBCO is restored because of the distortion of the lattice parameters relative to its idealized state due to the redistribution of the electron density around the nuclei, which differs from the electron density in neutral atoms. The stability of the crystal structure, like any structure, is determined by the rules (L. Pauling), which provide the polarization capacity of ions [56] and their screening. The collectivization of charge excitations and their relaxation in such systems can be similar to the processes observed for classical conductors in terms of the fact of satisfiability of Ohm's law. This law for non-metallic conductors is satisfied in a quasi-static process. To interpret the temperature dependence of the resistance of strongly correlated electron systems, for example, HTSC the theory based on the concepts of the gas and Fermi-liquid models of collectivized electrons within the Drude-Bloch concept is non-applicable [7]. When interpreting the resistance of non-metals, preference is the given to the physically substantiated concept of charge spreading, which follows from Maxwell's equations based on empirical laws. Moreover, it turns out to be valid for classical conductors as well, if the concept of electric current determined by the Gauss theorem is taken into account. The contradiction associated with the direct and inverse resistance on relaxation time dependences within the Maxwell and Drude-Bloch concepts is removed [57] by taking into account the thermal deformation of the lattice. According to [56,58], dielectric screening of local inhomogeneity of ion charges within the YBCO unit cell is realized by changing the concentration of socialized charge excitations with insignificant lattice deformations. Compression of the lattice leads to an increase in the doping level as indicated by the relationship [59,60] of the oxygen content and the T_c value with a decrease in the $\boldsymbol{c}$ parameter.

The transition from the normal to the superconducting state and back in a magnetic field is accompanied by the jump in volume [61]. Despite the obviousness of such a jump, the change in volume is the neglected due to its smallness in the theory. However, according to Maxwell's equation:

$$\oint_\ell \boldsymbol{E} d\ell = \oint_S -\frac{1}{c}\frac{\partial \boldsymbol{\Phi}}{\partial t} = \frac{1}{c}\left(-S\frac{\partial \boldsymbol{B}}{\partial t} - \boldsymbol{B}\frac{\partial S}{\partial t}\right) \quad (3)$$

a change in magnetic flux implies a change not only in magnetic induction but also a change in the geometric dimensions of the sample over time directly during the transition. The reasoning about the inevitable capture of the magnetic field when the external field is reduced to zero follows from the fact that the presence of such a deformation is not taken into account. If we take into account $B\partial S/\partial t$ in expression (3), then for any path of transition to the superconducting state, the effect of a trapped magnetic field does not arise. The deformation of the lattice for any path of transition to the superconducting state in a magnetic field implies a change in the density of states at the Fermi level.

Thermodynamics of the processes in these systems is directly related to quantum electrodynamics of ECE formation by inducing them with appropriate lattice deformations. Understanding of the relationship between properties characterized by the considered by thermodynamics and quantum electrodynamics processes is revealed [62] when considering the correlation in the formation of YBCO properties. Authors [62] show the relationship between thermodynamic parameters such as heat capacity and the second critical field H_{c2} with an increase in the effective mass of quasiparticles – an increase in the measure of inertia of electrostatic fields depending on the doping of YBCO. Such changes lead to the formation of the stable ortho-I and ortho-II superconducting phases resulting from the formation of the corresponding densities of states on the Fermi surface.

5. Conclusion

The analysis of the formation of electrical resistance and lattice deformation of YBCO with predominantly ionic-covalent bonding between atoms performed above shows that the restructuring of the energy spectrum of the charge subsystem leading to a change in the absolute and relative values of conductivity occurs at insignificant deformations. A linear correlation of the temperature coefficients of electrical resistance and volumetric thermal expansion is found for this connection with a correlation coefficient of no less than 0.98 in the normal state. The onset of the superconducting transition for each superconducting phase determined by the temperature dependence of electrical resistance is accompanied by lattice compression, after which an increase in the volume in the region of the middle values of T_c of these phases occurs. Deviations of the coefficients of volumetric expansion from their zero values for each of the superconducting phases in the interval of the transition to the superconducting state, in contrast to the derivative of electrical resistance with respect to temperature, occur with a change in the sign. We have established the order of the "virtual phonon" energy to be $\sim 10^{-5}$ eV, which is more than 2 orders of magnitude lower than the energy for YBCO (0.04 eV) established by the Debye temperature in [63]. This is consistent with the condition of interaction of electrons via phonons, which underlies the BCS theory.

CRediT authorship contribution statement

A. E. Rabadanova: Writing – original draft, Methodology. **D. K. Palchaev:** Methodology, Conceptualization, Supervision. **V. S.**

Efimchenko: Investigation. **R. M. Emirov:** Investigation. **Sh. P. Faradzhev:** Investigation. **S. Kh. Gadzhimagomedov:** Investigation, Validation, Writing – review & editing, Supervision. **Zh. Kh. Murlieva:** Translation, Validation, Writing – review & editing, Supervision. **M. Kh. Rabadanov:** Validation, Writing – review & editing, Supervision. **S. V. Simonov:** Investigation. **A. M. Aliyev:** Investigation. **A. A. Antsiferova:** Translation. **M. E. Iskhakov:** Investigation. **N. M-R. Alikhanov:** Translation, Investigation.

Compliance with ethical standards

The work is performed in compliance with all ethical norms.

Declaration of Competing Interest

The authors declare that they have no known competing financial interests or personal relationships that could have appeared to influence the work reported in this paper.

Acknowledgments

The authors are grateful for financial support from State Assignments FZNZ-2020–0002, FZNZ-2025–0003 (development of the scenario of the nature of HTSC) and RFBR (Grant No. 20–32–90170). The studies were carried out using equipment from the Nan-otechnology Research Center of the Dagestan State University, Institute of Solid State Physics and Dagestan Federal Research Center of the Russian Academy of Sciences.

References

[1] K. Wang, H. Dong, D. Huang, H. Shang, B. Xie, Q. Zou, L. Zhang, C. Feng, H. Gu, F. Ding, Advances in second-generation high-temperature superconducting tapes and their applications in high-field magnets, Soft Sci. 2 (2022) 1–28.
[2] N.V. Porokhov, A.S. Kalabukhov, M.L. Chukharkin, A.G. Maresov, D.A. Khrykin, N. V. Klenov, O.V. Snigirev, The physical basis of the fabrication of the third generation of high_temperature superconducting wires on Quartz Substrates, Mosc. Univ. Phys. Bull. 70 (2015) 134–139.
[3] N.A. Tulina, A.A. Ivanov, Memristive properties of oxide-based high-temperature superconductors, J. Supercond. Nov. Magn. 33 (2020) 2279–2286.
[4] P. Krantz, M. Kjaergaard, F. Yan, T.P. Orlando, S. Gustavsson, W.D. Oliver, A quantum engineer's guide to superconducting qubits, Appl. Phys. Rev. 6 (2019) 021318, 58.
[5] V.A. Vozhakov, M.V. Bastrakova, N.V. Klenov, I.I. Soloviev, W.V. Pogosov, D. V. Babukhin, A.A. Zhukov, A.M. Satanin, State control in superconducting quantum processors, Phys. Uspekhi 65 (2022) 421–439.
[6] A.F. Kockum, F. Nori, Quantum bits with josephson junctions, in: fundamentals and frontiers of the josephson effect, 286, Springer Ser. Mater. S, 2019, pp. 703–741.
[7] N. Singh, Leading theories of the cuprate superconductivity: a critique, Physica C Superconductivity Applications 580 (2021) 1353782, 9.
[8] S.I. Vedeneev, The pseudogap problem in high-temperature superconductors, Uspekhi Fiz. Nauk 191 (2021) 937–972.
[9] C.M. Varma, Colloquium: Linear in temperature resistivity and associated mysteries including high temperature superconductivity, Rev. Mod. Phys. 92 (2020) 031001–031015.
[10] A. Legros, S. Benhabib, W. Tabis, F. Laliberté, M. Dion, M. Lizaire, B. Vignolle, D. Vignolles, H. Raffy, Z.Z. Li, P. Auban-Senzier, N. Doiron-Leyraud, P. Fournier, D. Colson, L. Taillefer, C. Proust, Universal T-linear resistivity and Planckian dissipation in overtopped cuprates, Nat. Phys. 15 (2019) 142–147.
[11] P.W. Phillips, N.E. Hussey, P. Abbamonte, Stranger than metals, Science 377 (2022) 4273, 13.
[12] J.M. Ziman, Principles of the Theory of Solids, Cambridge university press, 1979.
[13] K. Ohta, Y. Kuwayama, K. Hirose, K. Shimizu, Y. Ohishi, Experimental determination of electrical resistivity of iron under conditions of the Earth's core, Nature 534 (2016) 95–98.
[14] S.V. Postolova, A.Yu Mironov, M.R. Baklanov, V.M. Vinokur, T.I. Baturina, Reentrant resistive behavior and dimensional crossover in disordered superconducting TiN films, Sci. Rep. 7 (2017) 1718, 7.
[15] J. Kim, M.W. Oh, S. Lee, Y.C. Cho, J.-H. Yoon, G.W. Lee, C.-R. Cho, C.H. Park, S.-Y. Jeong, Abnormal drop in electrical resistivity with impurity doping of single-crystal Ag, Sci. Rep. 4 (2014) 5450–5455.
[16] M. Bednarski, J. Chmist, P. Stochand, J. Pszczoła, Electrical resistivity, Curie temperature and band structure of $Ho(Fe_{1-x}Co_x)_2$ compounds, Phys. Scr. 85 (2012) 035703–035708.
[17] A.M. Pereira, J.P. Araujo, J.R. Peixoto, M.E. Braga, P.A. Algarabel, C. Magen, L. Morellon, M.R. Ibarra, J.B. Sousa, Electron scattering processes in $Ho_5(Si_xGe_{1-x})_4$ compounds: electrical resistivity studies, Phys. Rev. B 83 (2011) 144117–144118.
[18] D.K. Efetov, P. Kim, Controlling electron-phonon interactions in graphene at ultrahigh carrier densities, Phys. Rev. Lett. 105 (2010) 256805, 4.
[19] M.V. Kamalakar, A.K. Raychaudhuri, X. Wei, J. Teng, P.D. Prewett, Temperature dependent electrical resistivity of a single strand of ferromagnetic single crystalline nanowire, Appl. Phys. Lett. 95 (2009) 013112, 4.
[20] D.K. Palchaev, Z.K. Murlieva, K.K. Kazbekov, The correlation between electrical resistivity of metals and thermal deformation, High. Temp. 45 (2007) 632–638.
[21] Zh.Kh Murlieva, D.K. Palchaev, E.D. Borzov, M.E. Iskhakov, F.A. Akaev, The electrical resistance of nickel and ß-brass as a function of isobaric thermal deformation in ordered and disordered phases, High. Temp. 45 (2007) 797–802.
[22] Z.K. Murlieva, M.E. Iskhakov, D.K. Palchaev, M.P. Faradjeva, D.G. Chernykh, Temperature dependence of electrical resistance of alloys caused by dynamic and static disorders, High. Temp. 50 (2012) 602–610.
[23] D.K. Palchaev, Zh.Kh Murlieva, S.H. Gadzhimagomedov, M.E. Iskhakov, M. Kh Rabadanov, I.M. Abdulagatov, Thermal expansion and electrical resistivity studies of nickel and ARMCO iron at high temperatures, Int. J. Thermophys. 36 (2015) 3186–3210.
[24] D.K. Palchaev, Z.K. Murlieva, I.M. Abdulagatov, S.K. Gadzhimagomedov, M. E. Iskhakov, M.K. Rabadanov, Influence of magnetic properties on electric resistivity of iron-group elements, High. Temp. 55 (2017) 386–392.
[25] P.M. Horn, D.T. Keane, G.A. Held, J.L. Jordan-Sweet, D.L. Kaiser, F. Holtzberg, T. M. Rice, Orthorhombic distortion at the superconducting transition in $YBa_2Cu_3O_7$ evidence for anisotropic pairing, Phys. Rev. Lett. 59 (1987) 2772–2775.
[26] M. Francois, A. Junod, K. Yvon, A.W. Mewat, J.J. Capponi, P. Strobe, M. Marezio, P. Fischer, A Study of the Cu-O chains in the high T_c superconductor $YBa_2Cu_3O_7$ by high resolution neutron powder diffraction, Solid State Commun. 66 (1988) 1117–1125.
[27] H. You, U. Welp, Y. Fang, Slope discontinuity and fluctuation of lattice expansion near T_c in untwinned $YBa_2Cu_3O_{7-\delta}$ single crystals, Phys. Rev. B 43 (1991) 3660–3663.
[28] R.J. Cava, A.W. Hewat, E.A. Hewat, B. Batlogg, M. Marezio, K.M. Rabe, J. J. Krajewski, W.F. Peck Jr., L.W. Rupp, Jr., Structural anomalies, oxygen ordering and superconductivity in oxygen deficient $Ba_2YCu_3O_x$, Phys. C. 165 (1990) 419–433.
[29] R. Srinivasan, K.S. Girirajan, V. Ganesan, V. Radhakrishnan, G.S. Rao, Anomalous variation of the ***c*** lattice parameter of a sample of $YBa_2Cu_3O_{7-\delta}$ through the superconducting transition, Phys. Rev. B 38 (1988) 889–892.
[30] M. Lang, T. Lechner, S. Riegel, F. Steglich, G. Weber, T.J. Kim, M. Wilhelm, Thermal expansion, sound velocities, specific heat and pressure derivative of T_c in $YBa_2Cu_3O_7$, Z. Phys. B Condens. Matter 69 (1988) 459–463.
[31] C. Meingast, O. Kraut, T. Wolf, H. Wühl, A. Erb, G. Müller-Vogt, Large a-b anisotropy of the expansivity anomaly at T_c in untwinned $YBa_2Cu_3O_{7-\delta}$, Phys. Rev. Lett. 67 (1991) 1634–1637.
[32] W. Schnelle, E. Braun, H. Broicher, R. Dömel, S. Ruppel, W. Braunisch, D. Wohlleben, Fluctuation specific heat and thermal expansion of YBaCuO and DyBaCuO, Physica C Superconductivity 168 (1990) 465–474.
[33] V. Pasler, P. Schweiss, C. Meingast, B. Obst, H. Wühl, A.I. Rykov, S. Tajima, 3D−XY critical fluctuations of the thermal expansivity in detwinned $YBa_2Cu_3O_{7-\delta}$ single crystals near optimal doping, Phys. Rev. Lett. 81 (1998) 1094–1097.
[34] O. Kraut, C. Meingast, G. Bräuchle, H. Claus, A. Erb, G. Müller-Vogt, H. Wühl, Uniaxial pressure dependence of T_c of untwinned $YBa_2Cu_3O_x$ single crystals for x= 6.5–7, Physica C Superconductivity 205 (1993) 139–146.
[35] C. Meingast, V. Pasler, P. Nagel, A. Rykov, S. Tajima, P. Olsson, Phase fluctuations and the pseudogap in $YBa_2Cu_3O_x$, Phys. Rev. Lett. 86 (2001) 1606–1609.
[36] F. Hardy, P. Adelmann, T. Wolf, H. V. Löhneysen, C. Meingast, Large anisotropic uniaxial pressure dependencies of T_c in single crystalline $Ba(Fe_{0.92}Co_{0.08})_2As_2$, Phys. Rev. Lett. 102 (2009) 187004, 4.
[37] Y. Fujii, Y. Soejima, A. Okazaki, I.K. Bdikin, G.A. Emel'Chenko, A.A. Zhokhov, The characteristics of orthorhombicity of $YBa_2Cu_3O_{7-\delta}$ in superconducting state, Physica C Superconductivity 377 (2002) 49–55.
[38] M.S. da Luz, J.J. Neumeier, R.K. Bollinger, A.S. Sefat, M.A. McGuire, R. Jin, D. Mandrus, High-resolution measurements of the thermal expansion of superconducting Co-doped $BaFe_2As_2$, Phys. Rev. B 79 (2009) 214505, 6.
[39] A. Gasparini, Y.K. Huang, J. Hartbaum, H. V. Löhneysen, A. De Visser, Thermal expansion of the superconducting ferromagnet UCoGe, Phys. Rev. B 82 (2010) 052502, 4.
[40] J.J. Neumeier, T. Tomita, M. Debessai, J.S. Schilling, P.W. Barnes, D.G. Hinks, J. D. Jorgensen, Negative thermal expansion of MgB_2 in the superconducting state and anomalous behavior of the bulk Grüneisen function, Phys. Rev. B 72 (2005) 2205055, 4.
[41] Z.J. Yang, M. Yewondwossen, D.W. Lawther, S.P. Ritcey, D.J.W. Geldart, R. A. Dunlap, Thermal expansion of $Bi_{2.2}Sr_{1.8}CaCu_2O_x$ superconductor single crystals, J. Supercond. 8 (1995) 233–239.
[42] V. Palmisano, S. Agrestini, G. Campi, M. Filippi, L. Simonelli, M. Fratini, I. Margiolaki, Anomalous thermal expansion in superconducting $Mg_{1-x}Al_xB_2$ system, J. Supercond. 18 (2005) 737–741.
[43] W. Jin, S. Hao, H. Zhang, The fixed triangle chemical bond and its effect in the $Y_{1-x}Ca_xBa_{2-y}La_yCu_3O_z$ system from underdoped to overdoped, N. J. Phys. 11 (2009) 11303–11315.
[44] W.T. Jin, S.J. Hao, C.X. Wang, C.Q. Guo, L. Xia, S.L. Zhang, H. Zhang, Structural and spectroscopic evidence for stable chemical bonds and the correlation with high T_c superconductivity, Supercond. Sci. Technol. 25 (2012) 065004–065005.
[45] Q. Guo, C.Y. Zhang, S.J. Hao, W.T. Jin, H. Zhang, Fixed triangle in $Bi_{2-x}Pb_xSr_2CaCu_2O_{8+Y}$ and $Bi_{2-x}Pb_xSr_2Ca_2Cu_3O_{10+Y}$ systems, Int. J. Mod. Phys. B 27 (2013) 1362015.

[46] S.J. Hao, W.T. Jin, C.Q. Guo, H. Zhang, The stability of the CuO_2 plane and its influence on superconductivity in the doped $YBa_2Cu_3O_{7-\delta}$ system, Supercond. Sci. Technol. 26 (2013) 065011–065015.
[47] S.Kh Gadzhimagomedov, D.K. Palchaev, Zh.Kh Murlieva, M.Kh Rabadanov, M. Yu Presnyakov, E.V. Yastremsky, N.S. Shabanov, R.M. Emirov, A.E. Rabadanova, YBCO nanostructured ceramics: relationship between doping level and temperature coefficient of electrical resistance, J. Phys. Chem. Solids 168 (2022) 110811–110819.
[48] M.V. Sadovskii, Pseudogap in high-temperature superconductors, UFN 171 (2001) 539–564.
[49] D. Pelc, M.J. Veit, C.J. Dorow, Y. Ge, N. Barišíc, M. Greven, Resistivity phase diagram of cuprates revisited, Phys. Rev. B 102 (2020) 075114, 11.
[50] N. Barišic, M.K. Chana, Y. Lie, G. Yua, X. Zhaoa, M. Dressel, A. Smontara, M. Grevena, Universal sheet resistance and revised phase diagram of the cuprate high-temperature superconductors, PNAS 110 (2013) 12235–12240.
[51] K. Takenaka, K. Mizuhashi, H. Takagi, S. Uchida, Interplane charge transport in $YBa_2Cu_3O_{7-y}$ spin-gap effect on in-plane and out-of-plane resistivity, Phys. Rev. B 50 (1994) 6534–6537.
[52] W. Matz, L. Weiss, G. Schuster, E.S. Kuklina, Yu.Z. Nozik, Soviet, Phys. Crytallograph. 36 (1991) 125–126.
[53] H. Zhang, L.L. Cheng, X.C. Qin, Y. Zhao, Combinative energy between two structural blocks and its correlation with superconductivity in Bi and Hg superconducting systems, Phys. Rev. B 61 (2000) 1618–1622.
[54] J.C. Slater, Insulators, Semiconductors and Metals, McGraw-Hill, New York, 1967, p. 647.
[55] A.P. Menushenkov, A. Ivanov, V. Neverov, A. Lukyanov, A. Krasavin, A. A. Yastrebtsev, I.A. Kovalev, Y. Zhumagulov, A.V. Kuznetsov, V. Popov, G. Tselikov, I. Shchetinin, O. Krymskaya, A. Yaroslavtsev, R. Carley, L. Mercadier, Z. Yin, S. Parchenko, L.P. Hoang, N. Ghodrati, Y.Y. Kim, J. Schlappa, M. Izquierdo, S. Molodtsov, A. Scherz, Direct evidence of real-space pairing in $BaBiO_3$, Phys. Rev. Res. 6 (2024) 023307, 14.
[56] R.J. Cava, B. Batlogg, K.M. Rabe, E.A. Rietman, P.K. Gallagher, L.W. Rupp, Jr, Structural anomalies at the disappearance of superconductivity in $Ba_2YCu_3O_{7-\delta}$: evidence for charge transfer from chains to planes, Phys. C. 156 (1988) 523–527.
[57] D.K. Palchaev, Zh Kh Murlieva, M. Kh Rabadanov, S. Kh Gadzhimagomedov, M. E. Iskhakov, R.M. Emirov, Relationship between electrical resistance and thermal expansion coefficient in YBCO and $Ti_{67}Al_{33}$, J. Phys. Conf. 1686 (2020) 012051–012055.
[58] E.S. Bŏzin, A. Huq, B. Shen, H. Claus, W.K. Kwok, J.M. Tranquada, Charge-screening role of *c*-axis atomic displacements in $YBa_2Cu_3O_{6+x}$ and related superconductors, Phys. Rev. B 93 (2016) 054523, 11.
[59] R. Liang, D.A. Bonn, W.N. Hardy, Evaluation of CuO_2 plane hole doping in $YBa_2Cu_3O_{6+x}$ single crystals, Phys. Rev. B 73 (2006) 180505, 4.
[60] P. Benzi, E. Bottizzoa, N. Rizzi, Oxygen determination from cell dimensions in YBCO superconductors, J. Cryst. Growth 269 (2004) 625–629.
[61] E.A. Lynton, London, Methuen and Co. Ltd. New York. Superconductivity, John Wiley and Sons Inc, 1962.
[62] B.J. Ramshaw, S.E. Sebastian, R.D. McDonald, J. Day, B.S. Tan, Z. Zhu, J.B. Betts, R. Liang, D.A. Bonn, W.N. Hardy, N. Harrison, Quasiparticle mass enhancement approaching optimal doping in a high-Tc superconductor, Science 348 (2015) 317–320.
[63] L.K. Aminov, V.A. Ivanshin, I.N. Kurkin, M.R. Gafurov, I.Kh Salikhov, H. Keller, M. Gutmann, Debye temperature in $YBa_2Cu_3O_x$ as measured from the electron spin-lattice relaxation of doped Yb^{+3} ions, Phys. C Supercond. 349 (2001) 30–34.